Coherent manipulation of a Majorana qubit by a mechanical resonator

P. Zhang[1] and Franco Nori[1,2]
[1]*CEMS, RIKEN, Saitama 351-0198, Japan*
[2]*Department of Physics, University of Michigan, Ann Arbor, Michigan 48109-1040, USA*

(Received 19 June 2015; published 4 September 2015)

We propose a hybrid system composed of a Majorana qubit and a nanomechanical resonator, implemented by a spin-orbit-coupled superconducting nanowire, using a set of static and oscillating ferromagnetic gates. The ferromagnetic gates induce Majorana bound states in the nanowire, which hybridize and constitute a Majorana qubit. Due to the oscillation of one of these gates, the Majorana qubit can be coherently rotated. By tuning the gate voltage to modulate the local spin-orbit coupling, it is possible to reach the resonance of the qubit-oscillator system for relatively strong couplings.

DOI: 10.1103/PhysRevB.92.115303 PACS number(s): 71.10.Pm, 07.10.Cm

I. INTRODUCTION

Majorana bound states (MBS) [1,2] have been attracting increasing interest both theoretically and experimentally. They have been predicted to exist in artificial structures such as nanowires with spin-orbit coupling (SOC) in proximity to a superconductor [3,4], ferromagnetic atom chains on top of a superconductor [5], topological insulator/superconductor hybrid structures [6–11], and superconducting circuits [12]. Recently, possible signatures of MBS have been reported in nanowires [13–15], atom chains [16], and topological insulator/superconductor structures [17]. The MBS attract considerable attention partly due to their hypothetical non-Abelian anyonic statistics, which might allow the realization of topologically protected quantum information manipulation [2,18–20]. In parallel to the ongoing search of some unambiguous confirmation of MBS [21,22], there are also numerous theoretical studies on how to efficiently exploit these MBS.

One promising application of MBS is to construct Majorana qubits [18]. It has been suggested that Majorana qubits might be robust against local perturbations and are hence promising to store quantum information [18,23,24]. (Note that Majorana qubits are not totally protected from decoherence, as studied in, e.g., Refs. [25–28].) Furthermore, Majorana qubits could be rotated by topologically protected braiding operations [19,29]. Therefore, among various realizations of qubits [30–36], Majorana qubits are considered to be promising candidates for building blocks of quantum information processors. The braiding operations alone are insufficient to realize a universal quantum gate based on a Majorana qubit [18]. For the implementation of arbitrary qubit rotations, other nontopological operations are required. Several schemes of such nontopological operations assisted by, e.g., phase gates [37,38], quantum dots [39,40], flux qubits [41,42], or microwave cavities [43], have been proposed in the literature.

Nanomechanical resonators [44] could also be used to study nontopological operations of a Majorana qubit. For example, recently, Kovalev *et al.* [45] have proposed to rotate a Majorana qubit by a magnetic cantilever. Indeed, nanomechanical resonators have been utilized to couple to a wide range of quantum systems, including electric circuits [46], optomechanical devices [47], atoms [48], Cooper-pair boxes [49], spin qubits [50], and microwave cavities [51]. With the assistance of nanomechanical resonators, it is possible to perform important applications such as quantum manipulations, quantum measurements, and efficient sensing. These applications exploit the advantages of nanomechanical resonators, e.g., their large quality factors (10^3–10^6), high natural frequencies (MHz–GHz), and the feasibility of reaching the quantum ground states by cooling methods [52–54]. Recently, nanomechanical resonators have also been exploited to measure or manipulate the MBS [55–57]. Nevertheless, the study of hybrid systems [58] coupling nanomechanical resonators to Majorana qubits is quite limited. This work aims to contribute to this field. In this paper we propose another Majorana qubit-nanomechanical resonator hybrid system in the framework of the spin-boson model [59], based on a semiconductor nanowire in proximity to an s-wave superconductor. We show that a strong coupling between a nanomechanical resonator and a Majorana qubit can be achieved, allowing an efficient transfer of quantum information between these two quantum systems. Further, with braiding operations, it should be possible to realize a universal quantum gate based on a Majorana qubit.

This paper is organized as follows. First, we describe the Majorana qubit and its coupling to a nanomechanical resonator. Afterward, we numerically study the coupling strength and the resonance condition of the hybrid system. Then we solve the qubit-phonon dynamics and achieve a coherent control of the Majorana qubit. Finally, we summarize our results.

II. MODEL AND HAMILTONIAN

As illustrated in Fig. 1, we consider a semiconductor nanowire with a Rashba SOC of strength α_0^{R} on the surface of an s-wave superconductor with a superconducting gap Δ. Three ferromagnetic gates FM1, FM2, and FM3 are placed on top of and along the nanowire. Among these gates, FM1 and FM3 are static while FM2 is free to harmonically oscillate along the nanowire (with a mass M and an oscillation frequency ω_0). The gates FM1 and FM3 are sufficiently long (of the order of 1–10 μm) while FM2 in between is relatively short (of the order of 100 nm). These ferromagnetic gates induce a local Zeeman splitting in the nanowire. For simplicity, we take the Zeeman splitting under the three gates to be identical, with a magnitude of B_0. An electric voltage V can

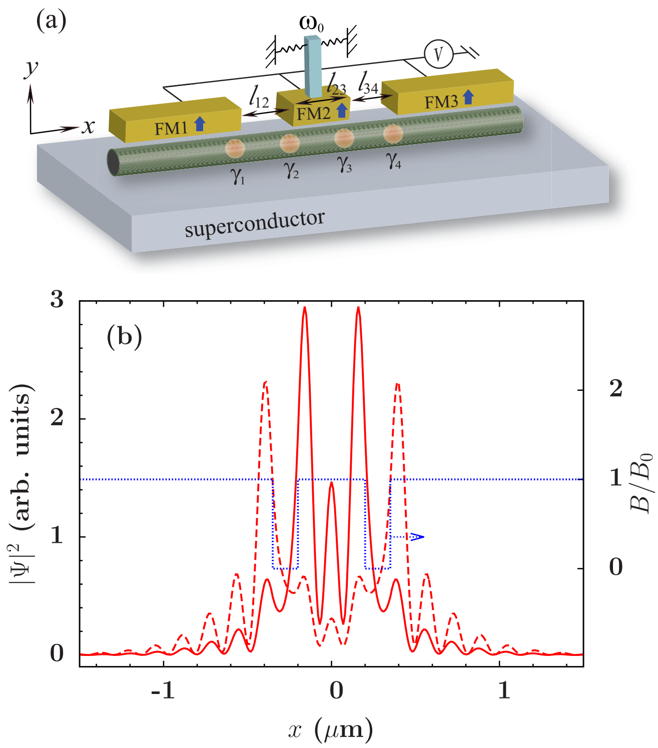

FIG. 1. (Color online) (a) Schematic diagram of the proposed Majorana qubit-nanomechanical resonator hybrid system. A semiconductor nanowire is placed on the surface of an s-wave superconductor. Three ferromagnetic gates are on top of the nanowire, of which FM1 and FM3 are sufficiently long (of the order of 1–10 μm) and static, while FM2 is relatively short (of the order of 100 nm) and free to oscillate as a harmonic oscillator. The ferromagnetic gates induce a local Zeeman splitting B_0 in the underlying nanowire and can also be used to modulate the local Rashba SOC strength by applying an electric voltage V. (b) Wave amplitude $|\Psi|^2$ of the four coupled MBS at a static state in an InSb nanowire with the setup shown in (a). The red dashed and red solid curves respectively correspond to the wave amplitudes of the lowest two eigenstates (close to zero energy). These two states constitute the Majorana qubit. The dotted curve with the scale on the right-hand side of the frame indicates the profile of the inhomogeneous Zeeman splitting along the nanowire. In the calculation $l_{12} = l_{34} = 150$ nm, $l_{23} = 400$ nm, $B_0 = 1$ meV, and $\Delta = 0.5$ meV. The gate voltage V is zero and the Rashba SOC is homogeneous along the nanowire, with a strength $\alpha_0^R = 20$ meV nm.

be applied on the gates to modulate the Rashba SOC locally, e.g., from α_0^R to α_V^R. In our study we consider the case with $B_0^2 > (\Delta^2 + \mu^2)$, where μ is the chemical potential in the nanowire. Therefore, in the nanowire, the parts subject to the Zeeman splitting (under the three ferromagnetic gates) are in the topological T region. The remaining parts, without the Zeeman splitting, are in the nontopological N region [4,19]. As a result, the nanowire has an N-T-N-T-N-T-N domain structure where the three T domains are under the gates. At the six boundaries between the N and T domains in the nanowire, MBS arise. As the two outer MBS are far apart, only the four inner ones, schematically labeled as γ_1–γ_4 in Fig. 1, are coupled due to hybridization arising from their small separation [60–63] and are hence relevant to our consideration.

To lowest order, the hybrid system constructed above can be described by the Hamiltonian

$$H = H_{\mathrm{M}} + H_{\mathrm{osc}}, \tag{1}$$

where the mutual coupling Hamiltonian of the MBS [60–63]

$$H_{\mathrm{M}} = ig_n[l_{12}(t)]\gamma_1\gamma_2 + ig_t(l_{23})\gamma_2\gamma_3 + ig_n[l_{34}(t)]\gamma_3\gamma_4 \tag{2}$$

and the nanomechanical oscillator Hamiltonian

$$H_{\mathrm{osc}} = \frac{p^2}{2M} + \frac{1}{2}M\omega_0^2 x_0^2(t). \tag{3}$$

The coupling strengths $g_{n,t}$ depend on the domain lengths l_{ij}. Due to the oscillation of the gate FM2, $l_{12}(t) = l_{12}^0 + x_0(t)$ and $l_{34}(t) = l_{34}^0 - x_0(t)$ are time dependent. Here $x_0(t)$ stands for the displacement of the gate FM2 from its balance position, which is much smaller than the static domain lengths $l_{12,34}^0$. Therefore, to first order in x_0 one has

$$\begin{aligned} H_{\mathrm{M}} = {} & i\big[g_n\big(l_{12}^0\big) + x_0(t)g_n'\big(l_{12}^0\big)\big]\gamma_1\gamma_2 + ig_t(l_{23})\gamma_2\gamma_3 \\ & + i\big[g_n\big(l_{34}^0\big) - x_0(t)g_n'\big(l_{34}^0\big)\big]\gamma_3\gamma_4. \end{aligned} \tag{4}$$

The four MBS, satisfying $\{\gamma_i,\gamma_j\} = \delta_{ij}$, can be used to construct a Majorana qubit as follows [2,18]. At first we define two Dirac fermion operators [64] $c_\uparrow = (\gamma_1 + i\gamma_4)/\sqrt{2}$ and $c_\downarrow = (\gamma_2 + i\gamma_3)/\sqrt{2}$. The Hilbert space of H_{M} can then be spanned by states $|n_\uparrow, n_\downarrow\rangle$, with the fermion occupation numbers $n_\uparrow = c_\uparrow^\dagger c_\uparrow$ and $n_\downarrow = c_\downarrow^\dagger c_\downarrow$. Due to the conservation of fermion parity, the states $\{|0,1\rangle, |1,0\rangle\}$ and $\{|0,0\rangle, |1,1\rangle\}$ form two decoupled (odd and even) sectors [2,41,43]. We assume that there is no high-energy excitation (e.g., no Cooper-pair breaking in the superconducting substrate) and restrict our study to the odd sector with $n_\uparrow + n_\downarrow = 1$. For convenience, we define pseudospins $|\Uparrow\rangle = |1,0\rangle$ and $|\Downarrow\rangle = |0,1\rangle$ and use them as the two logical states of the Majorana qubit [39,41,43,45]. In this pseudospin space, $i\gamma_1\gamma_2 = -i\gamma_3\gamma_4 = -\sigma_y$ and $i\gamma_2\gamma_3 = -\sigma_z$. The nanomechanical oscillator is quantized in the Fock space $\{|n\rangle\}$ with $|n\rangle = \frac{(a^\dagger)^n}{\sqrt{n!}}|0\rangle$, where $a = \sqrt{\frac{M\omega_0}{2\hbar}}(x_0 + \frac{i}{M\omega_0}p)$ is the annihilation operator of phonons. Consequently, in the space $\{|\Uparrow\Downarrow\rangle \otimes |n\rangle\}$, the hybrid system can be simply described by the spin-boson Hamiltonian [59]

$$H_{\mathrm{eff}} = -\frac{\varepsilon}{2}\sigma_z - \delta\sigma_y + g(a^\dagger + a)\sigma_y + n\hbar\omega_0, \tag{5}$$

with the constant omitted. Here $\varepsilon = 2g_t(l_{23})$, $\delta = g_n(l_{12}^0) - g_n(l_{34}^0)$, and $g = -\tilde{x}_0[g_n'(l_{12}^0) + g_n'(l_{34}^0)]$, where $\tilde{x}_0 = (\hbar/2M\omega_0)^{1/2}$ is the zero-point motion of the oscillator.

III. HYBRIDIZATION OF MAJORANA BOUND STATES

In this section we study the MBS and their mutual coupling. In the static state, the inhomogeneous nanowire can be described by a tight-binding model. Using the Bogoliubov-de Gennes basis $\Psi_j = (f_{j\uparrow}, f_{j\downarrow}, f_{j\downarrow}^\dagger, -f_{j\uparrow}^\dagger)$, where $f_{j\eta}$ stands for the fermion operator of a spin-η ($\eta = \uparrow,\downarrow$) electron on the jth lattice site, the particle-hole Hamiltonian reads [5]

$$H_{\mathrm{BDG}} = \frac{1}{2}\sum_j [\Psi_j^\dagger \hat{h}_j \Psi_j + (\Psi_j^\dagger \hat{t}_j \Psi_{j+1} + \mathrm{H.c.})], \tag{6}$$

where

$$\hat{h}_j = (2t_0 - \mu)s_0\tau_z + \Delta s_0\tau_x + B_j s_y \tau_0, \tag{7}$$

$$\hat{t}_j = t_0 s_0 \tau_z + i\alpha_j s_z \tau_z. \tag{8}$$

In the above Hamiltonian, the Pauli matrices $\tau_{x,y,z}$ act on the particle-hole space and $s_{x,y,z}$ act on the real spin space. The spin-diagonal hopping energy is $t_0 = \hbar^2/2m^*a^2$ and the spin–off-diagonal hopping energy is $\alpha_j = \alpha_j^{\rm R}/2a$. Here B_j and $\alpha_j^{\rm R}$ are the on-site Zeeman splitting and Rashba SOC, respectively, m^* is the effective electron mass, and a is the lattice spacing in the discretized tight-binding model. In the T (N) domains $B_j = B_0$ ($B_j = 0$) and $\alpha_j^{\rm R} = \alpha_V^{\rm R}$ ($\alpha_j^{\rm R} = \alpha_0^{\rm R}$). When the gate voltage V is zero, $\alpha_V^{\rm R} = \alpha_0^{\rm R}$.

Here, to lowest order, we follow Refs. [11,45] to investigate the coupling strength g_n (g_t) approximately in an isolated T-N-T (N-T-N) three-domain structure. In such a simplified model, the inner N (T) domain has a finite length, while the outer two T (N) domains are assumed to be infinitely long. By numerically diagonalizing this three-domain system, one can obtain the energy splitting of the two MBS localized at the two T/N boundaries. This energy splitting is precisely caused by the coupling of the MBS. With g_n and g_t known numerically, the Majorana qubit can be well described by ε and δ and the qubit-phonon coupling g can be obtained also from g_n' [refer to Eq. (5)]. Moreover, by exactly diagonalizing the Hamiltonian of the genuine N-T-N-T-N-T-N domain structure as shown in Fig. 1(a), one can obtain the four hybrid MBS under consideration.

In this work we consider an InSb quantum wire [13] with an effective electron mass $m^* = 0.015m_e$, a Rashba SOC $\alpha_0^{\rm R} =$ 20 meV nm, and a large Landau factor $g_L \approx 50$. We choose the superconducting gap $\Delta = 0.5$ meV, the local Zeeman splitting $B_0 = 1$ meV, the chemical potential $\mu = 0$, and the lattice constant $a = 10$ nm. The total lattice site number is chosen as 1000 for the numerical convergence. In Fig. 2 we show the dependence of the Majorana coupling strength g_n (g_t) on the length of the N (T) domain l_n (l_t), as well as the derivative g_n' versus l_n. Further, as an example, in Fig. 1(b) we present the wave amplitude $|\Psi|^2$ of the four hybrid MBS, when $l_{12} = l_{34} = 150$ nm and $l_{23} = 400$ nm. In Fig. 1(b) the red dashed and red solid curves stand for the wave amplitudes of the lowest two eigenstates (close to zero energy) in the static inhomogeneous nanowire. The state corresponding to the red solid (dashed) curve is mainly contributed by the γ_2 and γ_3 (γ_1 and γ_4) MBS. Here these two states form the Majorana qubit.

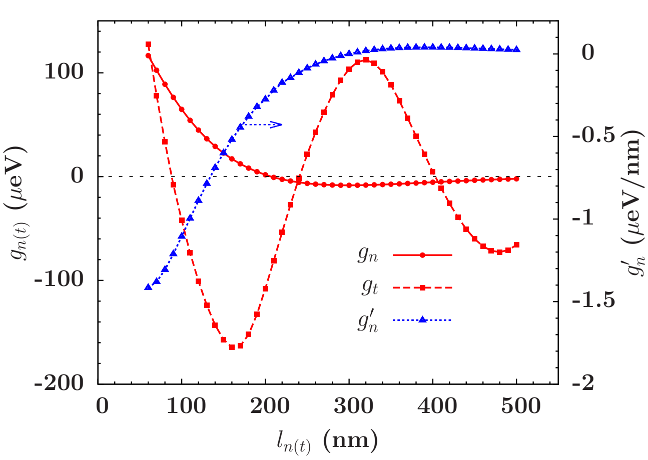

FIG. 2. (Color online) Majorana coupling strength g_n (g_t) versus l_n (l_t), the length of the inner N (T) domain between the two outer T (N) domains. The derivative g_n' versus l_n is also shown, with the scale on the right-hand side of the frame. The necessary parameters for the calculation are specified in the main text.

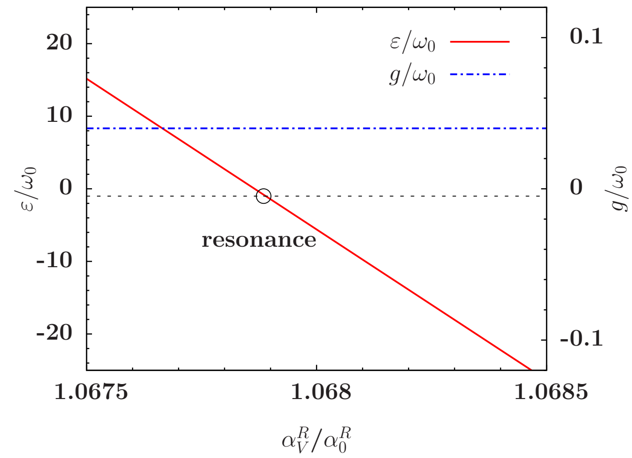

FIG. 3. (Color online) Qubit splitting ε and the qubit-phonon coupling g (the scale is on the right-hand side of the frame) versus $\alpha_V^{\rm R}$, the Rashba SOC strength in the topological T domains modulated by the gate voltage V.

IV. QUBIT-PHONON COUPLING AND RESONANCE

We now look into the qubit-phonon coupling and the resonance condition. We assume that the nanomechanical oscillator FM2 has a mass $M = 10^{-15}$ Kg and an oscillation frequency $\omega_0 = 5$ MHz. With these parameters, the zero-point motion of the oscillator is calculated to be $\tilde{x}_0 = 0.1$ pm. We consider the symmetric case with $l_{12}^0 = l_{34}^0 = 150$ nm and hence we have $\delta = 0$ and $g = 0.2$ MHz in Eq. (5). The longitudinal length l_{23} of the FM2 gate is chosen as 400 nm such that the Rabi resonance condition $\varepsilon \approx -\omega_0$ can be easily satisfied, e.g., by further subtly adjusting the gate voltage V that controls the local Rashba SOC strength $\alpha_V^{\rm R}$. In Fig. 3 we present the variation of ε as well as g versus $\alpha_V^{\rm R}$. It is shown that when slightly adjusting V, and hence $\alpha_0^{\rm R}$, the resonance point $\varepsilon \approx -\omega_0$ can be reached while the qubit-phonon coupling g remains almost invariant. This qubit-phonon coupling is relatively strong, in view of the long lifetime of the Majorana qubit and the high quality factor of the nanomechanical oscillator. In principle, the qubit-phonon coupling can be stronger when the domain length l_{12} (as well as l_{34}) becomes smaller (refer to Fig. 2). However, if the two edge modes γ_1 and γ_2 (as well as γ_3 and γ_4) are too close and hence their hybridization becomes quite strong, the model Hamiltonian (2) describing four distinguishable MBS might fail.

V. QUBIT-PHONON DYNAMICS

Here we study the dynamics of the qubit-phonon hybrid system. To achieve this, we make use of the Python-based QUTIP software package [65,66] to solve the Lindblad master equation

$$\dot{\rho}(t) = -\frac{i}{\hbar}[H_{\text{eff}},\rho(t)] + \frac{1}{2}\sum_k \{[L_k,\rho(t)L_k^\dagger] + [L_k\rho(t),L_k^\dagger]\}. \quad (9)$$

In this equation ρ is the density matrix of the qubit-phonon system and L_k are the Lindblad operators accounting for the dissipation of the hybrid system due to its coupling to the environment. The relaxation of the Majorana qubit is taken into account by $L_1 = \sqrt{1/T_1}\sigma_-$, while the dissipation of the nanomechanical resonator is included by $L_2 = \sqrt{(\bar{n}+1)\omega_0/Q}a$ and $L_3 = \sqrt{\bar{n}\omega_0/Q}a^\dagger$. Here $\bar{n} = [\exp(\hbar\omega_0/k_B\tilde{T}) - 1]^{-1}$ is the thermal phonon number in equilibrium with the environmental temperature $\tilde{T}$, Q is the quality factor of the nanomechanical oscillator, and T_1 is the usual relaxation time of the qubit. By solving the master equation, one can obtain the time evolution of the qubit and phonon occupations.

In our model the temperature $\tilde{T}$ is set as 10 mK and hence the thermal phonon number $\bar{n}$ is as large as 258. Therefore, an additional cooling of the oscillator [52–54] is required, e.g., as also applied in a proposed nanomechanical resonator–nitrogen-vacancy center hybrid system [51]. We assume that after sideband cooling [52–54] the phonons thermally occupy the lowest several quantum states with a small phonon number, e.g., $n = 0.3$. The initial state of the Majorana qubit is set as $|\uparrow\rangle$, implying that a single electron is split into the γ_1 and γ_4 Majorana fermions. Experimentally, this initial state might be realized when only the FM1 and FM3 gates are in proximity to the nanowire before inserting the middle FM2 gate. The relaxation time of the Majorana qubit depends on the concrete setup and environment. Following Refs. [26,27], we typically set T_1 around 100 μs.

In Fig. 4 we plot the time evolution of the occupations of the qubit and phonons, respectively, with different values of T_1 and Q. As indicated by the figure, quantum information can be effectively transferred back and forth between the Majorana qubit and the nanomechanical resonator. During this process, the single electron in the nanowire alternatively occupies (back and forth) the pair of MBS: γ_1 and γ_4, or γ_2 and γ_3. Inversely, this quantum information transfer can also modulate the motion of the oscillator, e.g., the oscillation amplitude. In fact, as the nanomechanical resonator is near its quantum ground state, the oscillation amplitude $\langle x_0^2\rangle$, which might be observable, is almost linearly related to the phonon number. This is because $\langle x_0^2\rangle \propto \langle(a^\dagger + a)^2\rangle \approx 2\langle a^\dagger a\rangle + 1 = 2n + 1$. Therefore, the dashed curves in Fig. 4, representing the time evolution of the phonon number, also supply information on the change of the oscillation amplitude of the resonator due to its coupling with the qubit. This phenomenon signifies the presence of a Majorana qubit. Certainly, for better performance of this hybrid system (e.g., with a higher fidelity), a higher quality factor of the resonator and a longer relaxation time of the qubit are preferred.

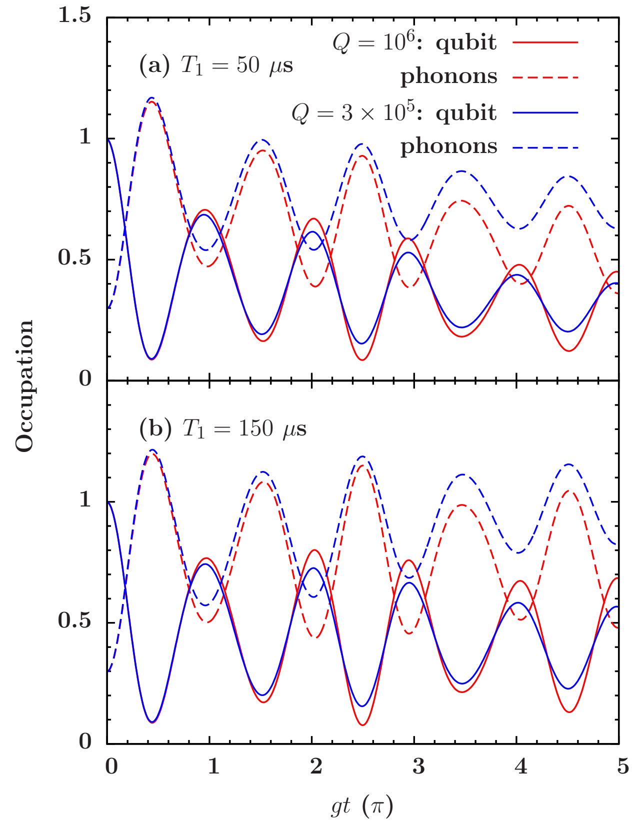

FIG. 4. (Color online) Time evolution of the occupations of the Majorana qubit (solid curves) and phonons (dashed curves), which are in Rabi resonance. The qubit relaxation time is set as (a) 50 μs and (b) 150 μs. The calculations for both (a) and (b) are performed with two different resonator quality factors: $Q = 10^6$ and $Q = 3 \times 10^5$.

VI. DISCUSSION

Here we briefly compare our model to the one proposed by Kovalev *et al.* [45], where a vibrating cantilever is utilized to rotate a Majorana qubit. The effective Hamiltonian in their model [Eq. (7) in Ref. [45]] is in fact equivalent to the one in our paper [Eq. (5)]. This is understandable as both are in the framework of the spin-boson model. Note that for both cases there exists a static off-diagonal term [for our case, it is the δ term in Eq. (5)] coupling the two levels of the qubit in the Hamiltonian. To neglect this term, in order to simplify the theoretical analysis, some conditions have to be satisfied. Specifically, in Ref. [5], a certain equilibrium angle (θ_0 therein) of the vibrating cantilever has to be established. In our opinion, exactly solving this angle and then adjusting the experimental setup correspondingly [45] are challenging. However, in order to neglect the constant off-diagonal term in our case, the experimental setup must be mirror symmetric about the middle point of the FM2 gate, i.e., $l_{12}^0 = l_{34}^0$. Therefore, we think that our model is more easily accessible by experiments and hence more advantageous.

VII. CONCLUSION

We have proposed a hybrid system composed of a Majorana qubit and a mechanical resonator, implemented by a semiconductor nanowire in proximity to an s-wave superconductor. In this proposal, three ferromagnetic gates are placed on top of and along the nanowire; the two outer gates are static and the inner one is free to oscillate harmonically as a mechanical resonator. These ferromagnetic gates induce a local Zeeman splitting and give rise to four Majorana bound states, constituting a Majorana qubit in the nanowire. The dynamical hybridization of the Majorana bound states, arising from the motion of the oscillating gate, results in a coherent coupling between the Majorana qubit and the mechanical resonator.

This hybrid system can be adjusted to be in resonance, e.g., with the assistance of a gate voltage on the ferromagnetic gates, which controls the Rashba SOC locally in the nanowire. Our study reveals that under resonance, a strong coupling between the qubit and the resonator can be achieved. Consequently, quantum information can be effectively transferred from the Majorana qubit to the oscillator and then back to the qubit. This quantum information transfer can manifest itself in modulating the motion of the oscillator, which may conversely signify the presence of the Majorana qubit.

ACKNOWLEDGMENTS

The authors gratefully acknowledge X. Hu, G. Giavaras, L. Wang, and Z. Li for valuable discussions and comments. P.Z. acknowledges the support of a JSPS Foreign Postdoctoral Fellowship under Grant No. P14330. F.N. was partially supported by the RIKEN iTHES Project, MURI Center for Dynamic Magneto-Optics via the AFOSR Grant No. FA9550-14-1-0040, the IMPACT program of JST, and a Grant-in-Aid for Scientific Research (A).

[1] A. Y. Kitaev, Unpaired Majorana fermions in quantum wires, Phys. Usp. **44**, 131 (2001).

[2] C. W. J. Beenakker, Search for Majorana fermions in superconductors, Annu. Rev. Condens. Matter Phys. **4**, 113 (2013).

[3] R. M. Lutchyn, J. D. Sau, and S. Das Sarma, Majorana Fermions and a Topological Phase Transition in Semiconductor-Superconductor Heterostructures, Phys. Rev. Lett. **105**, 077001 (2010).

[4] Y. Oreg, G. Refael and F. von Oppen, Helical Liquids and Majorana Bound States in Quantum Wires, Phys. Rev. Lett. **105**, 177002 (2010).

[5] T. P. Choy, J. M. Edge, A. R. Akhmerov, and C. W. J. Beenakker, Majorana fermions emerging from magnetic nanoparticles on a superconductor without spin-orbit coupling, Phys. Rev. B **84**, 195442 (2011).

[6] L. Fu and C. L. Kane, Superconducting Proximity Effect and Majorana Fermions at the Surface of a Topological Insulator, Phys. Rev. Lett. **100**, 096407 (2008).

[7] A. Cook and M. Franz, Majorana fermions in a topological-insulator nanowire proximity-coupled to an s-wave superconductor, Phys. Rev. B **84**, 201105 (2011).

[8] A. L. Rakhmanov, A. V. Rozhkov, and F. Nori, Majorana fermions in pinned vortices, Phys. Rev. B **84**, 075141 (2011).

[9] R. S. Akzyanov, A. V. Rozhkov, A. L. Rakhmanov, and F. Nori, Tunneling spectrum of a pinned vortex with a robust Majorana state, Phys. Rev. B **89**, 085409 (2014).

[10] R. S. Akzyanov, A. L. Rakhmanov, A. V. Rozhkov, and F. Nori, Majorana fermions at the edge of superconducting islands, Phys. Rev. B **92**, 075432 (2015).

[11] L. Jiang, D. Pekker, J. Alicea, G. Refael, Y. Oreg, A. Brataas, and F. von Oppen, Magneto-Josephson effects in junctions with Majorana bound states, Phys. Rev. B **87**, 075438 (2013).

[12] J. Q. You, Z. D. Wang, W. Zhang, and F. Nori, Encoding a qubit with Majorana modes in superconducting circuits, Sci. Rep. **4**, 5535 (2014).

[13] V. Mourik, K. Zuo, S. M. Frolov, S. R. Plissard, E. P. A. M. Bakkers, and L. P. Kouwenhoven, Signatures of Majorana fermions in hybrid superconductor semiconductor nanowire devices, Science **336**, 1003 (2012).

[14] M. T. Deng, C. L. Yu, G. Y. Huang, M. Larsson, P. Caroff, and H. Q. Xu, Anomalous zero-bias conductance peak in a Nb-InSb nanowire-Nb hybrid device, Nano Lett. **12**, 6414 (2012).

[15] A. Das, Y. Ronen, Y. Most, Y. Oreg, M. Heiblum, and H. Shtrikman, Zero-bias peaks and splitting in an AlInAs nanowire topological superconductor as a signature of Majorana fermions, Nat. Phys. **8**, 887 (2012).

[16] S. N. Perge, I. K. Drozdov, J. Li, H. Chen, S. Jeon, J. Seo, A. H. MacDonald, B. A. Bernevig, and A. Yazdani, Observation of Majorana fermions in ferromagnetic atomic chains on a superconductor, Science **346**, 602 (2014).

[17] J. P. Xu, M. X. Wang, Z. L. Liu, J. F. Ge, X. J. Yang, C. H. Liu, Z. A. Xu, D. Guan, C. L. Gao, D. Qian, Y. Liu, Q. H. Wang, F. C. Zhang, Q. K. Xue, and J. F. Jia, Experimental Detection of a Majorana Mode in the Core of a Magnetic Vortex Inside a Topological Insulator-Superconductor $Bi_2Te_3/NbSe_2$ Heterostructure, Phys. Rev. Lett. **114**, 017001 (2015).

[18] C. Nayak, S. H. Simon, A. Stern, M. Freedman, and S. Das Sarma, Non-Abelian anyons and topological quantum computation, Rev. Mod. Phys. **80**, 1083 (2008).

[19] J. Alicea, Y. Oreg, G. Refael, F. von Oppen, and M. P. A. Fisher, Non-Abelian statistics and topological quantum information processing in 1D wire networks, Nat. Phys. **7**, 412 (2011).

[20] S. Tewari, S. Das Sarma, C. Nayak, C. Zhang, and P. Zoller, Quantum Computation Using Vortices and Majorana Zero Modes of a $p_x + ip_y$ Superfluid of Fermionic Cold Atoms, Phys. Rev. Lett. **98**, 010506 (2007).

[21] J. Liu, A. C. Potter, K. T. Law, and P. A. Lee, Zero-Bias Peaks in the Tunneling Conductance of Spin-Orbit-Coupled Superconducting Wires with and without Majorana End-States, Phys. Rev. Lett. **109**, 267002 (2012).

[22] E. Dumitrescu, B. Roberts, S. Tewari, J. D. Sau, and S. Das Sarma, Majorana fermions in chiral topological ferromagnetic nanowires, Phys. Rev. B **91**, 094505 (2015).

[23] L. Mao and C. Zhang, Robustness of Majorana modes and minigaps in a spin-orbit-coupled semiconductor-superconductor heterostructure, Phys. Rev. B **82**, 174506 (2010).

[24] J. D. Sau and S. Das Sarma, Realizing a robust practical Majorana chain in a quantum-dot-superconductor linear array, Nat. Commun. **3**, 964 (2012).

[25] G. Goldstein and C. Chamon, Decay rates for topological memories encoded with Majorana fermions, Phys. Rev. B **84**, 205109 (2011).

[26] D. Rainis and D. Loss, Majorana qubit decoherence by quasi-particle poisoning, Phys. Rev. B **85**, 174533 (2012).

[27] M. J. Schmidt, D. Rainis, and D. Loss, Decoherence of Majorana qubits by noisy gates, Phys. Rev. B **86**, 085414 (2012).

[28] J. C. Budich, S. Walter, and B. Trauzettel, Failure of protection of Majorana based qubits against decoherence, Phys. Rev. B **85**, 121405 (2012).

[29] D. A. Ivanov, Non-Abelian Statistics of Half-Quantum Vortices in p-Wave Superconductors, Phys. Rev. Lett. **86**, 268 (2001).

[30] M. W. Wu, J. H. Jiang, and M. Q. Weng, Spin dynamics in semiconductors, Phys. Rep. **493**, 61 (2010).

[31] S. N. Perge, S. M. Frolov, E. P. A. M. Bakkers, and L. P. Kouwenhoven, Spin-orbit qubit in a semiconductor nanowire, Nature (London) **468**, 1084 (2010).

[32] P. Zhang, Z. L. Xiang, and F. Nori, Spin-orbit qubit on a multiferroic insulator in a superconducting resonator, Phys. Rev. B **89**, 115417 (2014).

[33] R. Li, J. Q. You, C. P. Sun, and F. Nori, Controlling a Nanowire Spin-Orbit Qubit Via Electric-Dipole Spin Resonance, Phys. Rev. Lett. **111**, 086805 (2013).

[34] I. Buluta and F. Nori, Quantum simulators, Science **326**, 108 (2009).

[35] I. Buluta, S. Ashhab, and F. Nori, Natural and artificial atoms for quantum computation, Rep. Prog. Phys. **74**, 104401 (2011).

[36] J. Q. You and F. Nori, Atomic physics and quantum optics using superconducting circuits, Nature (London) **474**, 589 (2011).

[37] P. Bonderson, D. J. Clarke, C. Nayak, and K. Shtengel, Implementing Arbitrary Phase Gates with Ising Anyons, Phys. Rev. Lett. **104**, 180505 (2010).

[38] D. J. Clarke and K. Shtengel, Improved phase-gate reliability in systems with neutral Ising anyons, Phys. Rev. B **82**, 180519 (2010).

[39] K. Flensberg, Non-Abelian Operations on Majorana Fermions Via Single-Charge Control, Phys. Rev. Lett. **106**, 090503 (2011).

[40] P. Bonderson and R. M. Lutchyn, Topological Quantum Buses: Coherent Quantum Information Transfer Between Topological and Conventional Qubits, Phys. Rev. Lett. **106**, 130505 (2011).

[41] D. Pekker, C. Y. Hou, V. E. Manucharyan, and E. Demler, Proposal for Coherent Coupling of Majorana Zero Modes and Superconducting Qubits Using the 4π Josephson Effect, Phys. Rev. Lett. **111**, 107007 (2013).

[42] F. Hassler, A. R. Akhmerov, C. Y. Hou, and C. W. J. Beenakker, Anyonic interferometry without anyons: How a flux qubit can read out a topological qubit, New J. Phys. **12**, 125002 (2010).

[43] T. L. Schmidt, A. Nunnenkamp, and C. Bruder, Majorana Qubit Rotations in Microwave Cavities, Phys. Rev. Lett. **110**, 107006 (2013).

[44] H. G. Craighead, Nanoelectromechanical systems, Science **290**, 1532 (2000).

[45] A. A. Kovalev, A. De, and K. Shtengel, Spin Transfer of Quantum Information Between Majorana Modes and a Resonator, Phys. Rev. Lett. **112**, 106402 (2014).

[46] M. Blencowe, Quantum electromechanical systems, Phys. Rep. **395**, 159 (2004).

[47] M. Aspelmeyer, T. J. Kippenberg, and F. Marquardt, Cavity optomechanics, Rev. Mod. Phys. **86**, 1391 (2014).

[48] K. Hammerer, M. Wallquist, C. Genes, M. Ludwig, F. Marquardt, P. Treutlein, P. Zoller, J. Ye, and H. J. Kimble, Strong Coupling of a Mechanical Oscillator and a Single Atom, Phys. Rev. Lett. **103**, 063005 (2009).

[49] E. K. Irish and K. Schwab, Quantum measurement of a coupled nanomechanical resonator-Cooper-pair box system, Phys. Rev. B **68**, 155311 (2003).

[50] P. Rabl, P. Cappellaro, M. V. Gurudev Dutt, L. Jiang, J. R. Maze, and M. D. Lukin, Strong magnetic coupling between an electronic spin qubit and a mechanical resonator, Phys. Rev. B **79**, 041302 (2009).

[51] P. B. Li, Y. C. Liu, S. Y. Gao, Z. L. Xiang, P. Rabl, F. L. Li, and Y. F. Xiao, Hybrid quantum device based on NV centers in diamond nanomechanical resonators plus superconducting waveguide cavities, arXiv:1503.02437.

[52] A. D. O'Connell, M. Hofheinz, M. Ansmann, R. C. Bialczak, M. Lenander, E. Lucero, M. Neeley, D. Sank, H. Wang, M. Weides, J. Wenner, J. M. Martinis, and A. N. Cleland, Quantum ground state and single-phonon control of a mechanical resonator, Nature (London) **464**, 697 (2010).

[53] J. D. Teufel, T. Donner, D. Li, J. W. Harlow, M. S. Allman, K. Cicak, A. J. Sirois, J. D. Whittaker, K. W. Lehnert, and R. W. Simmonds, Sideband cooling of micromechanical motion to the quantum ground state, Nature (London) **475**, 359 (2011).

[54] J. Chan, T. P. M. Alegre, A. H. S. Naeini, J. T. Hill, A. Krause, S. Gröblacher, M. Aspelmeyer, and O. Painter, Laser cooling of a nanomechanical oscillator into its quantum ground state, Nature (London) **478**, 89 (2011).

[55] S. Walter, T. L. Schmidt, K. Børkje, and B. Trauzettel, Detecting Majorana bound states by nanomechanics, Phys. Rev. B **84**, 224510 (2011).

[56] S. Walter and J. C. Budich, Teleportation-induced entanglement of two nanomechanical oscillators coupled to a topological superconductor, Phys. Rev. B **89**, 155431 (2014).

[57] H. J. Chen and K. D. Zhu, All-optical scheme for detecting the possible Majorana signature based on QD and nanomechanical resonator systems, Sci. China Phys. Mech. Astron. **58**, 050301 (2015).

[58] Z. L. Xiang, S. Ashhab, J. Q. You, and F. Nori, Hybrid quantum circuits: Superconducting circuits interacting with other quantum systems, Rev. Mod. Phys. **85**, 623 (2013).

[59] A. J. Leggett, S. Chakravarty, A. T. Dorsey, M. P. A. Fisher, A. Garg, and W. Zwerger, Dynamics of the dissipative two-state system, Rev. Mod. Phys. **59**, 1 (1987).

[60] C. J. Bolech and E. Demler, Observing Majorana Bound States in p-Wave Superconductors Using Noise Measurements in Tunneling Experiments, Phys. Rev. Lett. **98**, 237002 (2007).

[61] G. W. Semenoff and P. Sodano, Stretched quantum states emerging from a Majorana medium, J. Phys. B **40**, 1479 (2007).

[62] S. Tewari, C. Zhang, S. Das Sarma, C. Nayak, and D.-H. Lee, Testable Signatures of Quantum Nonlocality in a Two-Dimensional Chiral p-Wave Superconductor, Phys. Rev. Lett. **100**, 027001 (2008).

[63] Y. E. Kraus, A. Auerbach, H. A. Fertig, and S. H. Simon, Testing for Majorana Zero Modes in a $p_x + ip_y$ Superconductor at High Temperature by Tunneling Spectroscopy, Phys. Rev. Lett. **101**, 267002 (2008).

[64] Note that the pairing of MBS to form Dirac fermions is arbitrary. A given pairing defines a basis and different bases can be connected by a unitary transformation [18]. Here we define Dirac fermions according to the initial state where a single electron is split into a pair of Majorana fermions γ_1 and γ_4 (refer to Sec. V).

[65] J. R. Johansson, P. D. Nation, and F. Nori, QuTiP: A python framework for the dynamics of open quantum systems, Comput. Phys. Commun. **183**, 1760 (2012).

[66] J. R. Johansson, P. D. Nation, and F. Nori, QuTiP. 2: A python framework for the dynamics of open quantum systems, Comput. Phys. Commun. **184**, 1234 (2013).